Supporting Information

Multiroom-structured multicomponent metal selenide-graphitic carbon-carbon nanotube hybrid microspheres as efficient anode materials for sodium-ion batteries

Gi Dae Park, Yun Chan Kang*

Department of Materials Science and Engineering, Korea University, Anam-dong, Seongbuk-gu, Seoul 136-713, Republic of Korea

E-mail: yckang@korea.ac.kr Fax: +82-2-928-3584; Tel: +82-2-3290-3268

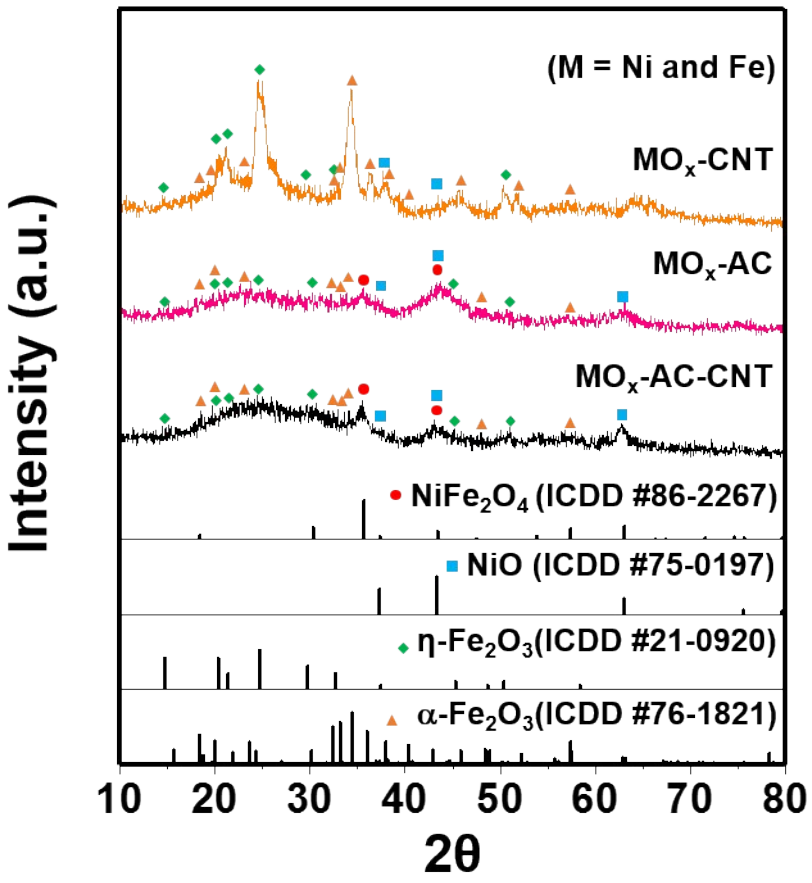

Fig. S1 XRD patterns of MO_x-AC-CNT (M=Ni and Fe), MO_x-AC, and MO_x-CNT hybrid microspheres directly formed by spray pyrolysis.

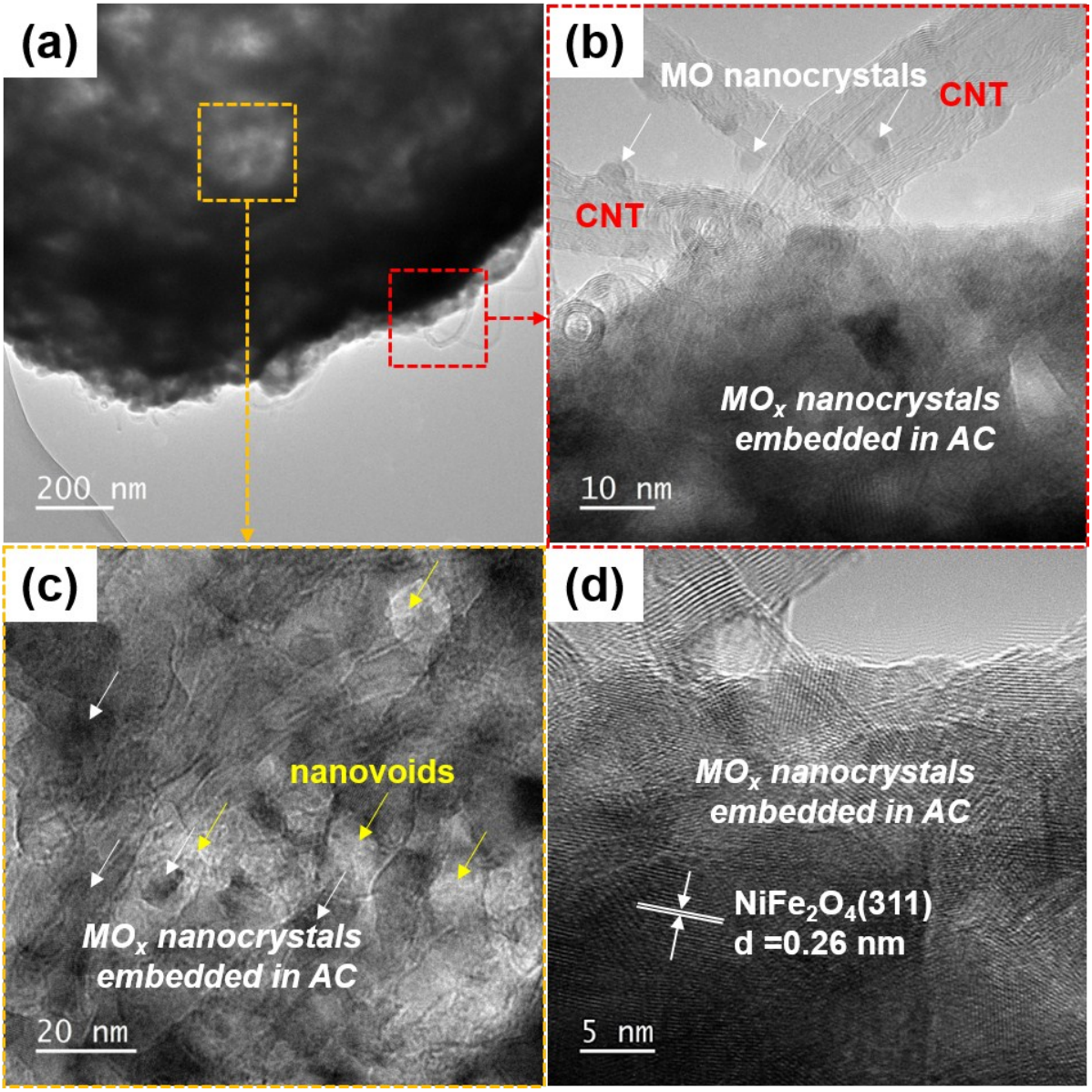

Fig. S2 TEM images of multiroom-structured MOx-AC-CNT hybrid microspheres.

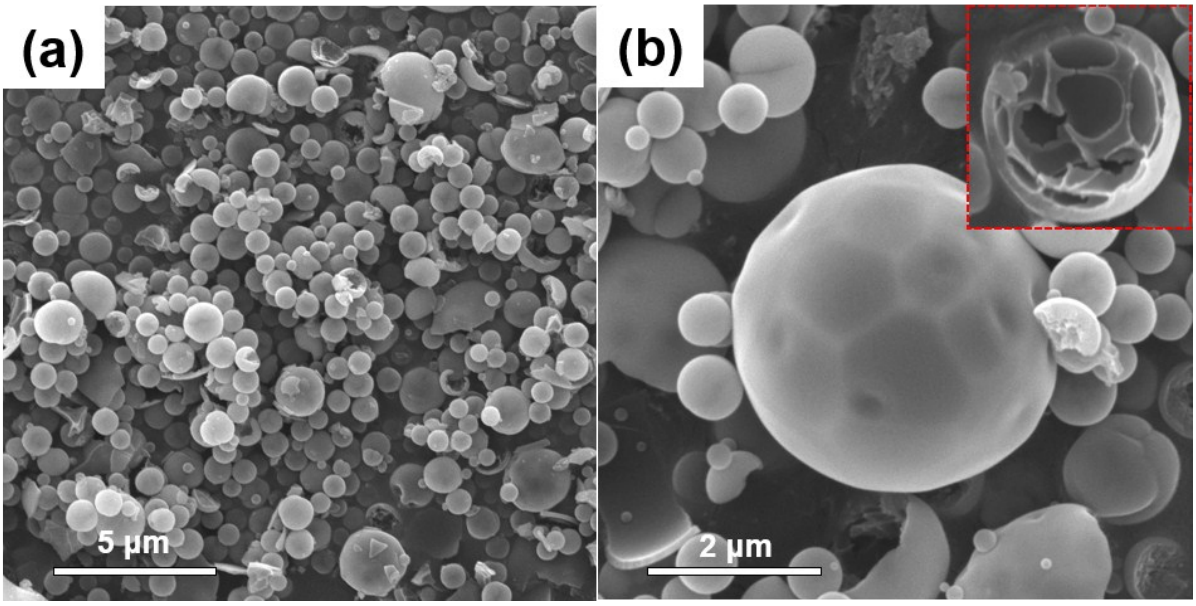

Fig. S3 SEM images of the MO_x-AC (M=Ni and Fe) microspheres directly prepared by spray pyrolysis.

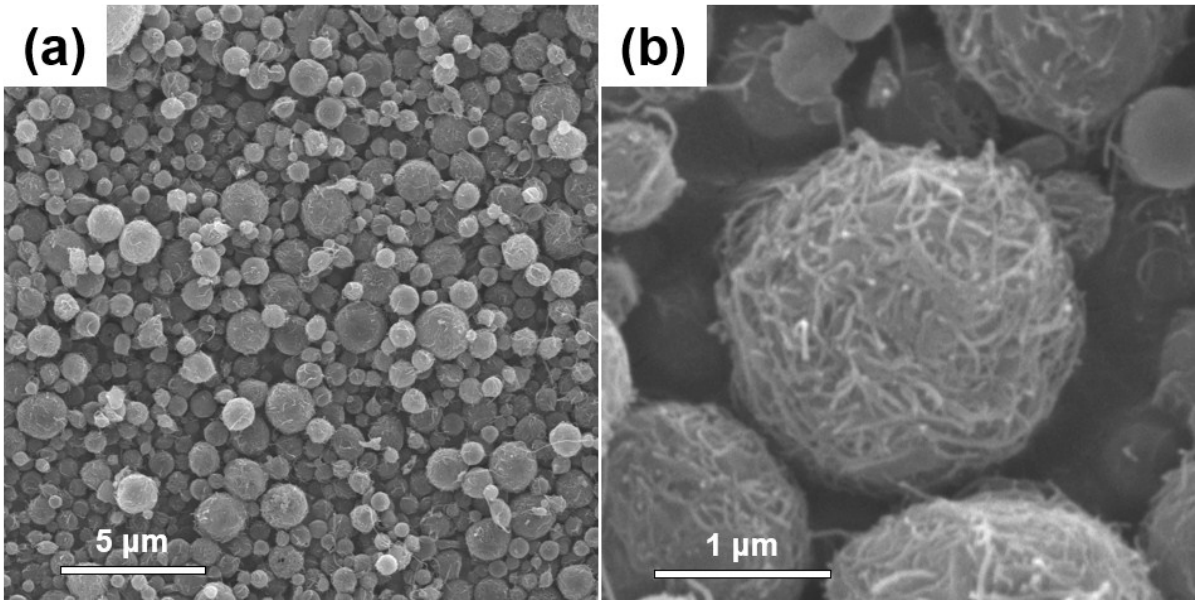

Fig. S4 SEM images of the MO_x-CNT (M=Ni and Fe) microspheres directly prepared by spray pyrolysis.

.

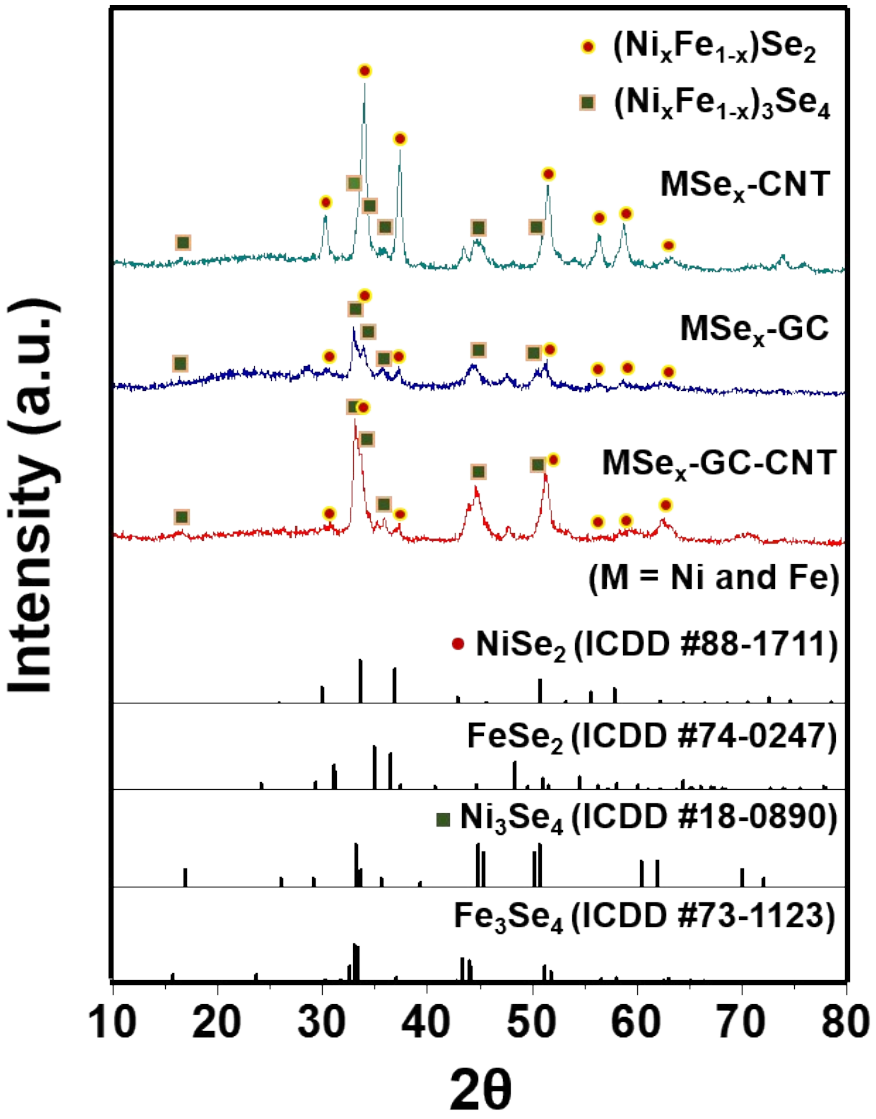

Fig. S5 XRD patterns of MSe_x-GC-CNT (M=Ni and Fe), MSe_x-GC, and MSe_x-CNT hybrid microspheres formed by spray pyrolysis and subsequent one-step post-treatment.

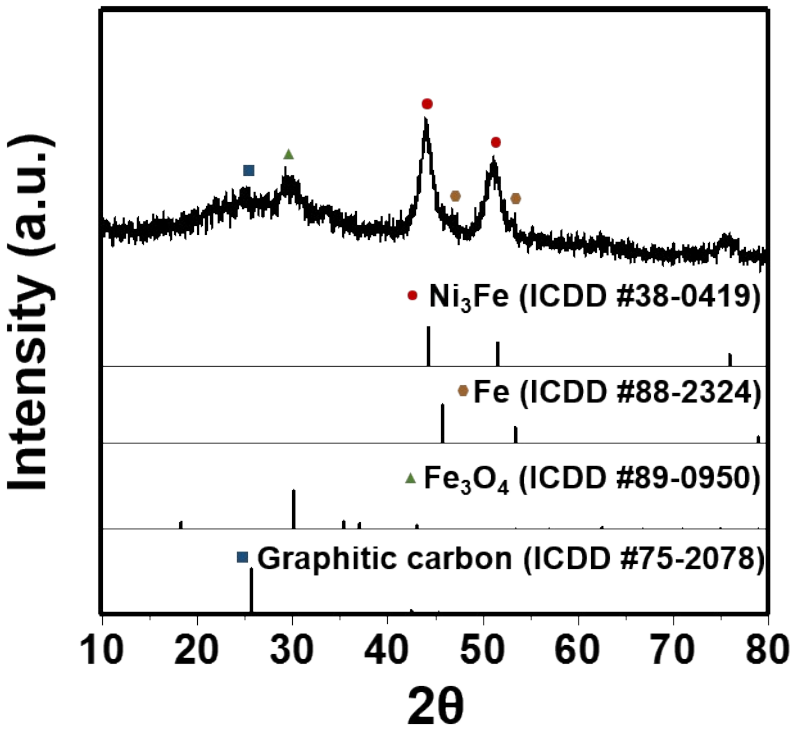

Fig. S6 XRD pattern of metallic NiFe-GC-CNT hybrid microspheres obtained by post-treatment of $(NiFe)O_x$-AC-CNT microspheres at 300 °C under 10% H_2/Ar atmosphere.

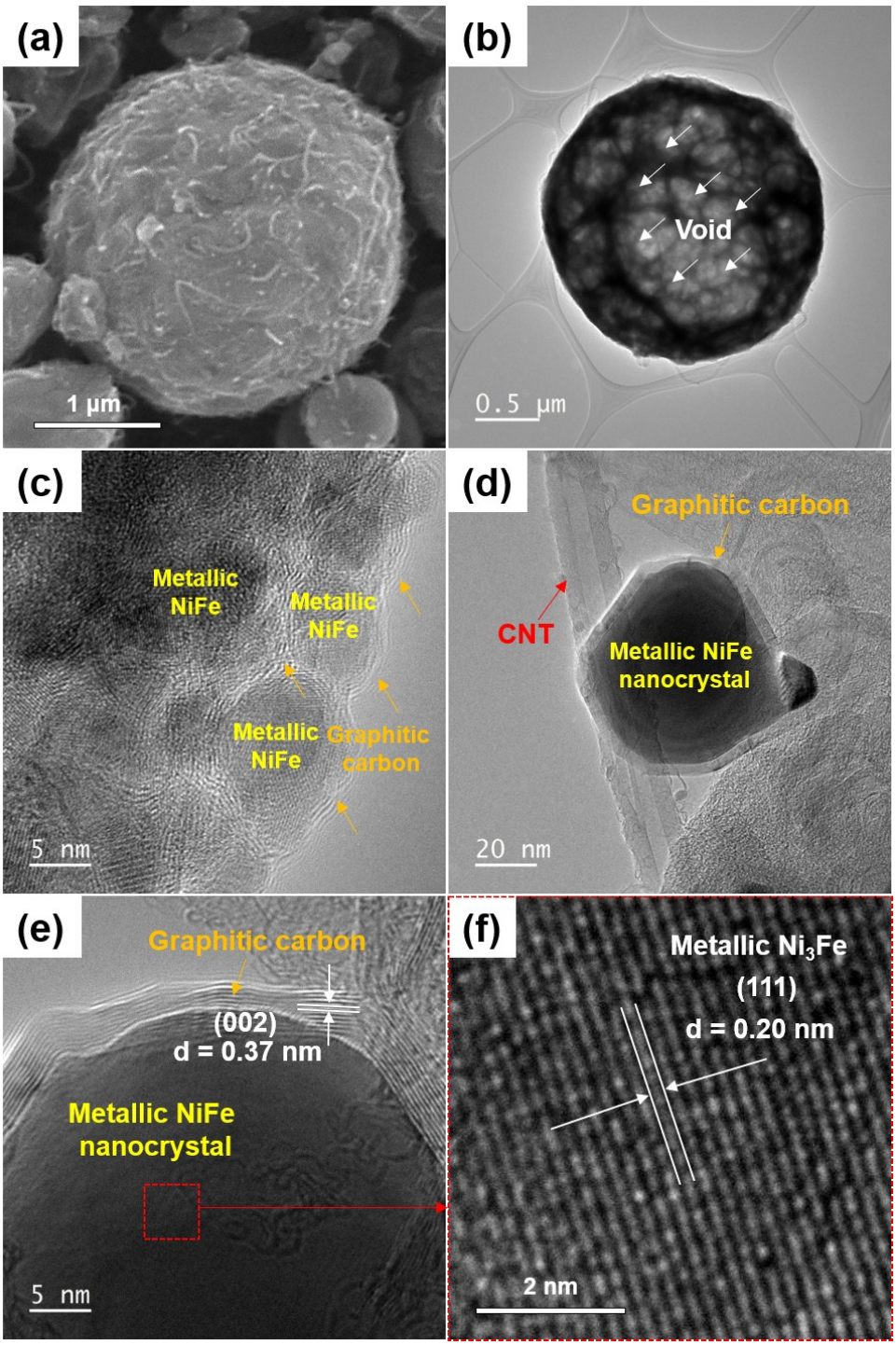

Fig. S7 Morphologies of metallic NiFe-GC-CNT hybrid microspheres obtained by post-treatment of (NiFe)O_x-AC-CNT microspheres without Se at 300 °C under 10% H_2/Ar atmosphere: (a) SEM, (b-d) TEM, and (e,f) high-resolution TEM images.

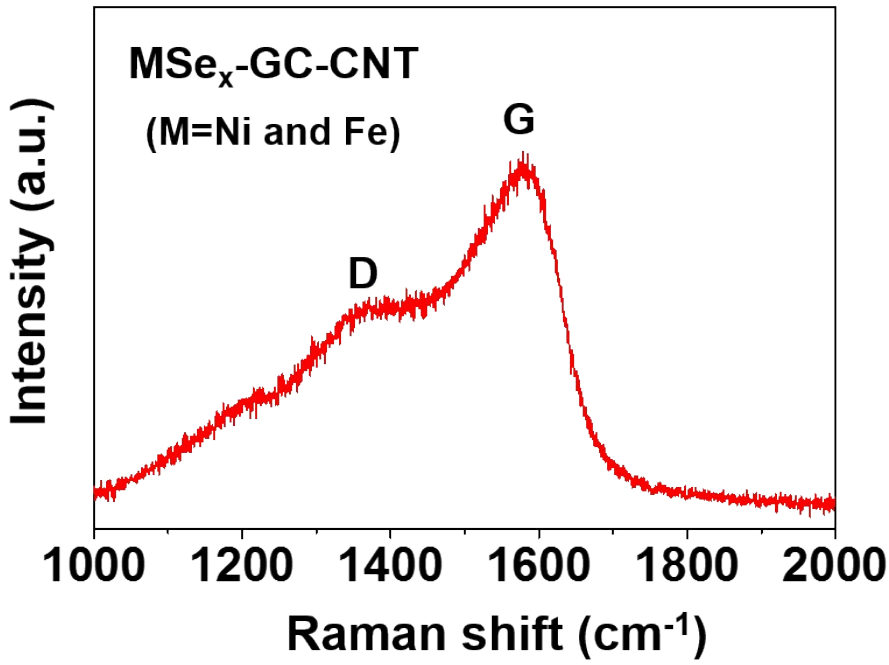

Fig. S8 Raman spectrum of MSe_x-GC-CNT (M=Ni and Fe) hybrid microspheres formed by spray pyrolysis and subsequent one-step post-treatment

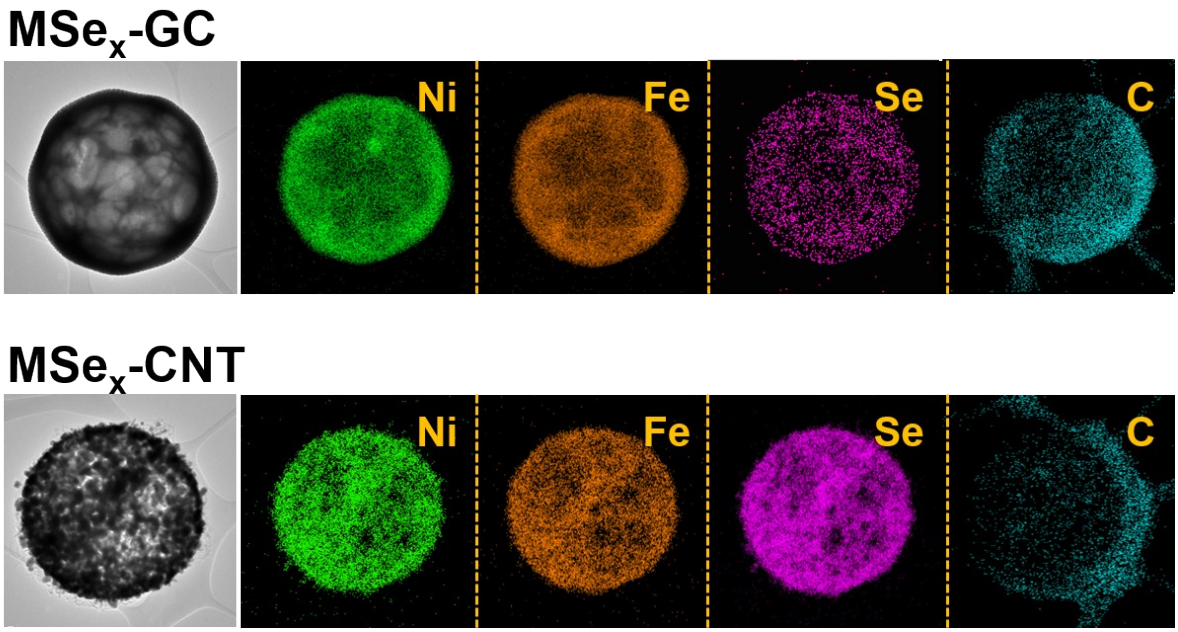

Fig. S9 Elemental mapping images of MSe_x-GC (M=Ni and Fe) and MSe_x-CNT hybrid microspheres formed by spray pyrolysis and subsequent one-step post-treatment.

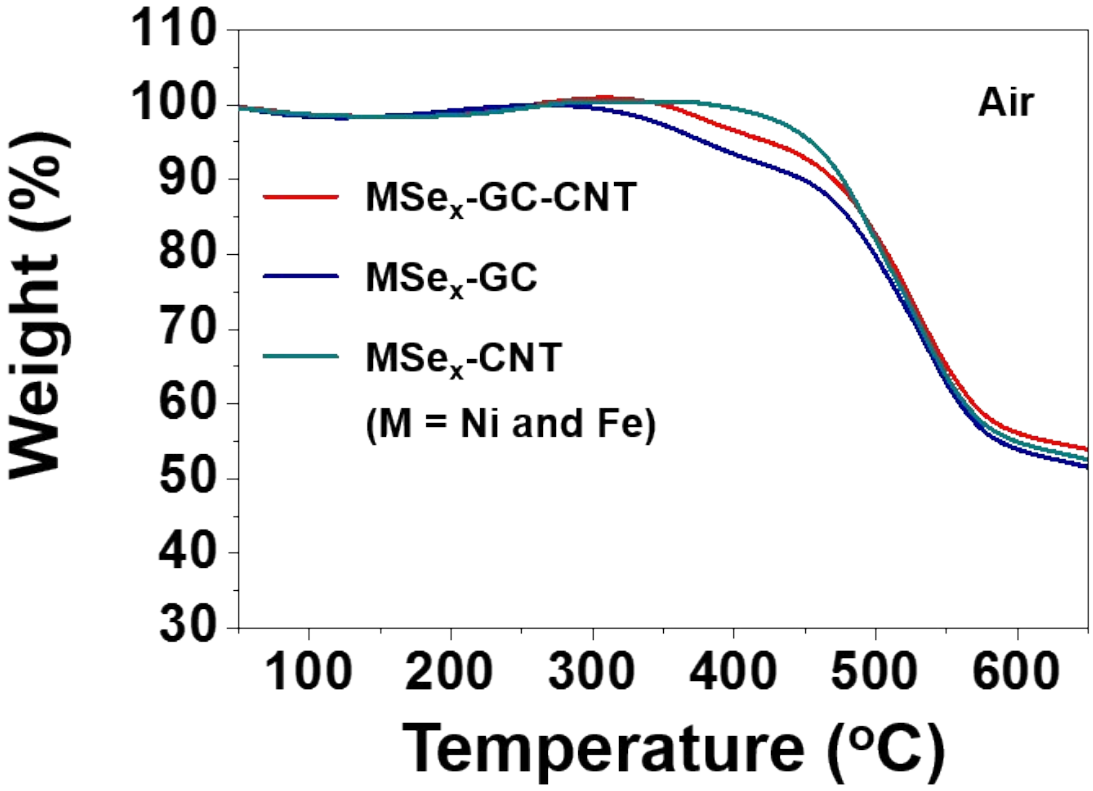

Fig. S10 TG curves of MSe_x-GC-CNT (M=Ni and Fe), MSe_x-GC, and MSe_x-CNT hybrid microspheres formed by spray pyrolysis and subsequent one-step post-treatment.

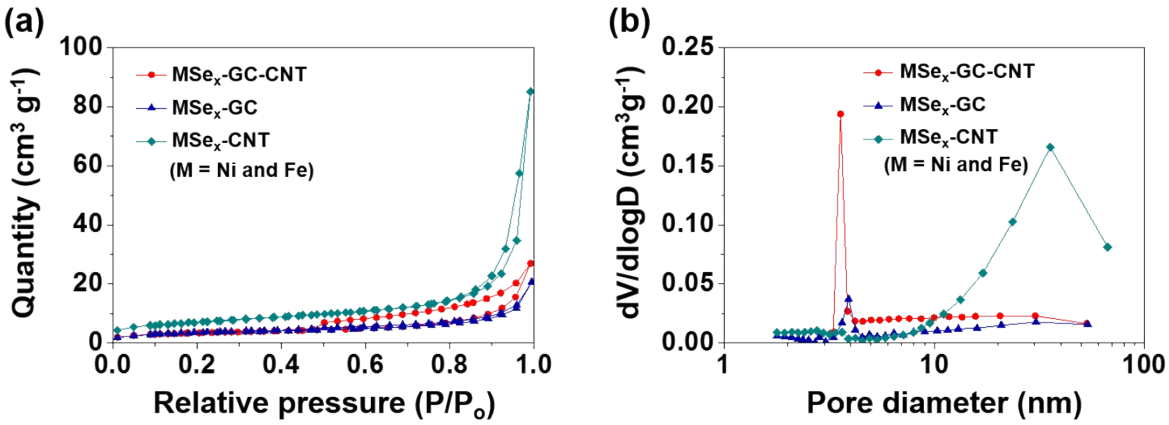

Fig. S11 (a) N_2 adsorption and desorption isotherms and (b) BJH pore size distributions of MSe_x-GC-CNT (M=Ni and Fe), MSe_x-GC, and MSe_x-CNT hybrid microspheres formed by spray pyrolysis and subsequent one-step post-treatment.

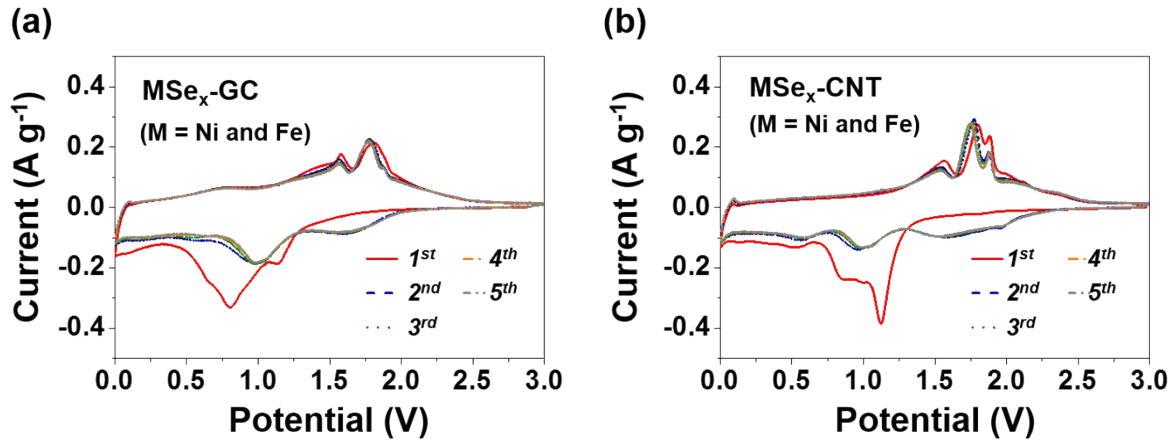

Fig. S12 CV curves of (a) MSe_x-GC (M=Ni and Fe) and (b) MSe_x-CNT hybrid microspheres formed by spray pyrolysis and subsequent one-step post-treatment.

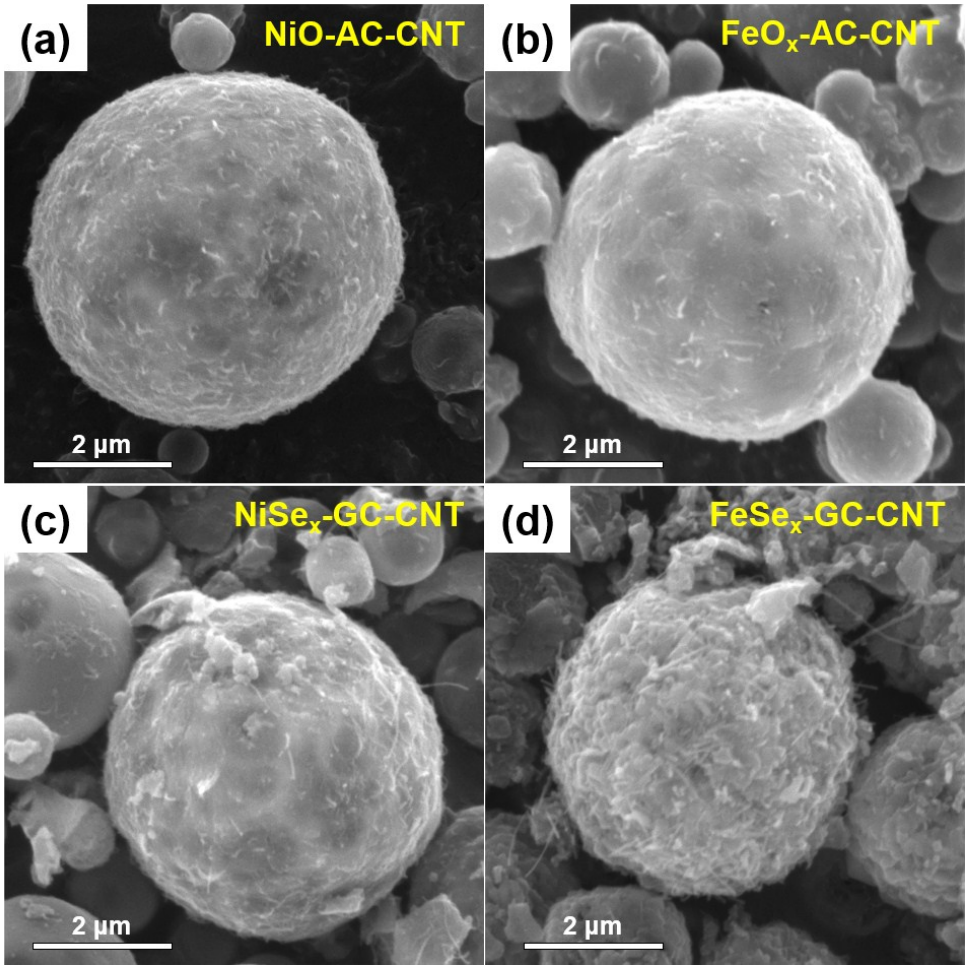

Fig. S13 Morphologies of (a) NiO-, (b) FeO_x-, (c) $NiSe_x$-, (d) and $FeSe_x$-GC-CNT hybrid microspheres.

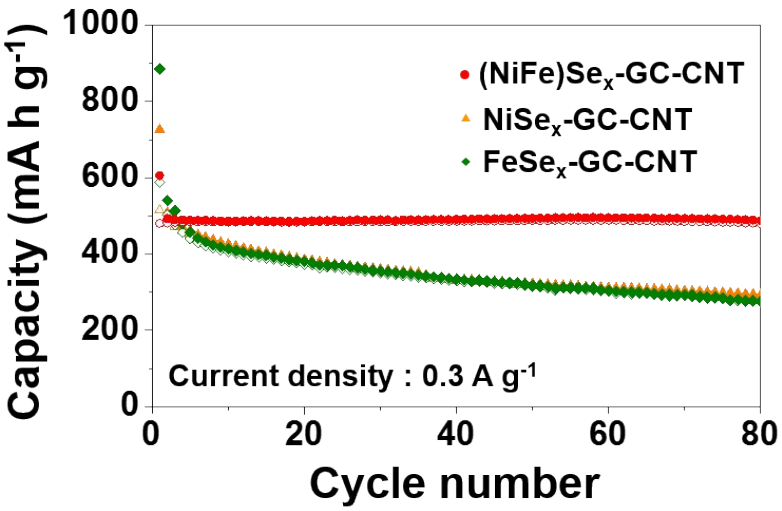

Fig. S14 Cycling performances of multiroom-structured (NiFe)Se_x-GC-CNT, $NiSe_x$-GC-CNT, $FeSe_x$-GC-CNT hybrid microspheres at a current density of 0.3 A g^{-1}.

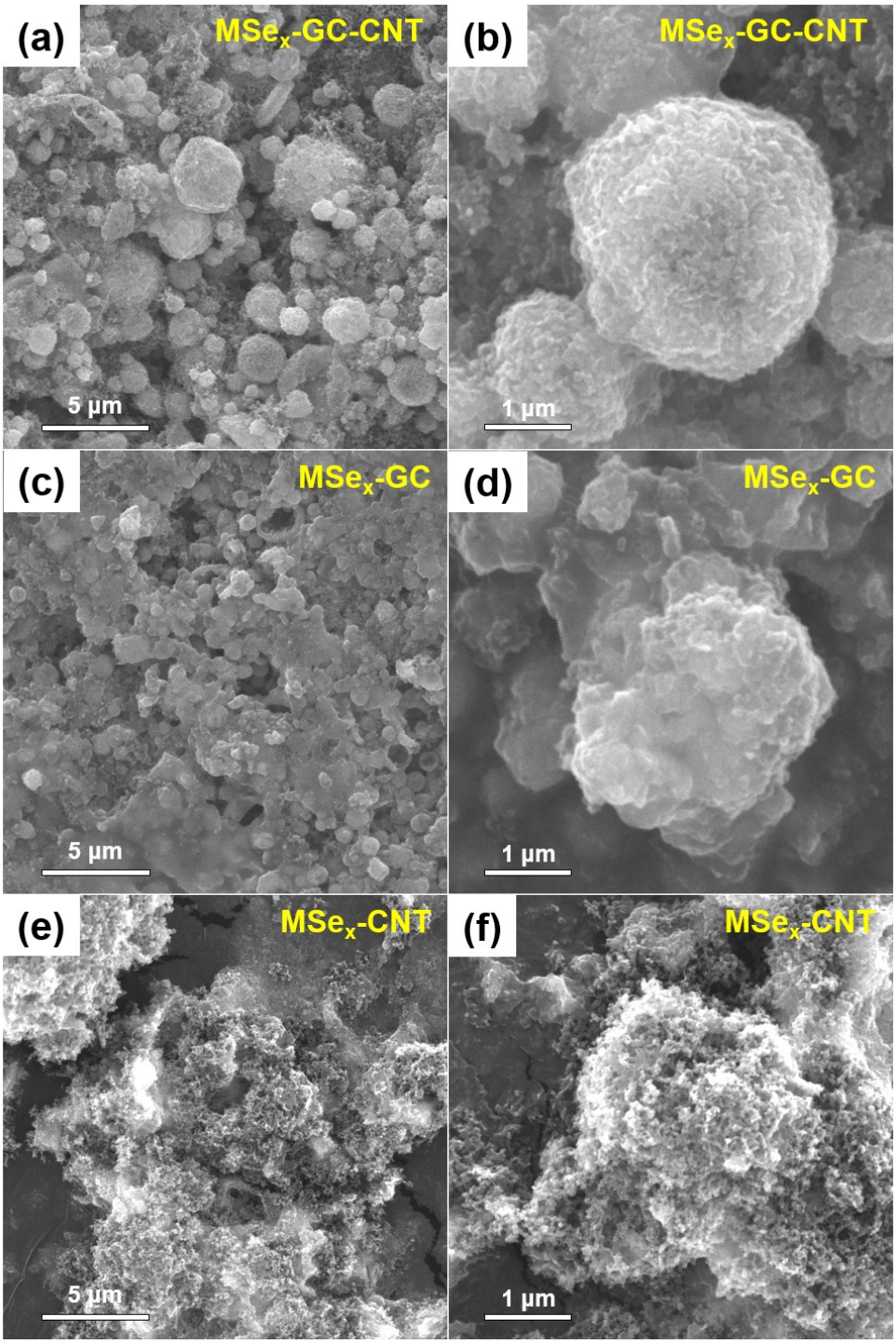

Fig. S15 SEM images of MSe_x-GC-CNT (M=Ni and Fe), MSe_x-GC, and MSe_x-CNT hybrid microspheres after 100 cycles: (a,b) MSe_x-GC-CNT, (c,d) MSe_x-GC, and (e,f) MSe_x-CNT.